Letters

An Optimized *dq*-Frame Admittance Modeling Method for Single-Phase Railway Vehicle-Grid System Considering the Impact of Asymmetric $\alpha\beta$ Control

Siqi Wu, *Member, IEEE*, Siqi Bu, *Senior Member, IEEE*, and Zhigang Liu, *Fellow, IEEE*

***Abstract*—To tackle the small-signal instability in the single-phase railway vehicle-grid system, the *dq* admittance modeling method has received great attention. However, the orthogonal β components created by the asymmetric quadrature signal generators (QSGs) for *dq* control inevitably suffer from amplitude or phase errors at nonfundamental frequencies, which are not fully considered in the traditional *dq* modeling method. As revealed in this letter, due to the inherent signal dimensionality reduction process from the actual control output (2-D scalar) to the single-phase power stage input (1-D scalar), the nonideal β components can introduce nonnegligible errors to the traditional *dq* model. Thus, as a solution, an optimized *dq* admittance modeling method for the single-phase converter in vehicles is proposed, which involves the impact of the asymmetric QSGs by capturing the signal dimensionality reduction process, based on the existing *dq* models. Furthermore, the stability analysis and hardware-in-the-loop (HIL) simulations are achieved, which verify the effectiveness of the proposed optimization methodology.**

***Index Terms*—*dq* admittance, oscillations, vehicle-grid system.**

I. Introduction

NOWADAYS, power electronic converters are increasingly used in the vehicles of modern railway systems. Their control interaction with the traction power grid (hereafter called grid) frequently leads to small-signal stability issues, necessitating system modeling and stability analysis. For this purpose, the *dq* admittance model is widely developed, since it can be easily obtained via linearization around the time-invariant operation points and intuitively characterize the dynamics of the commonly adopted *dq* controllers [1].

Although there is only one phase, the quadrature signal generation based phase-locked loop (PLL) and the *dq* current control are popularized in the single-phase converters, wherein the quadrature signal generators (QSGs) [2], such as the second-order generalized integrator (SOGI) and the transfer delay, play a key role in creating the orthogonal β components (the system original signals are regarded as α components). However, QSGs can only guarantee that the β components at fundamental frequency are ideal 90° lagging terms, whereas the amplitude or phase errors of the β components at nonfundamental frequencies will be inevitably caused (hereafter, this type of $\alpha\beta$ control is defined to be asymmetric). In other words, there is always a deviation between the created β components in the control system and the defined ideal β components in the *dq* modeling process at nonfundamental frequencies.

In [3], the imprecision of the derived *dq* model of a single-phase dynamic power compensator is observed around 50 Hz (refers to *dq* frame), and it is found that this imprecision mainly derives from two factors: 1) the neglect of the amplitude errors of β components (regarded as ideal) in the modeling process of SOGIs; and 2) the inconsistency of the duty ratio dynamics captured in the *dq* model and that input to the actual single-phase power stage of the compensator. To eliminate the impact of the first factor, the precise *dq* model of SOGI can be further derived by tracking the flow of the small-signal perturbations with amplitude errors in SOGI [2]. Nevertheless, the root cause of the error from the duty ratio part still remains unclear, which makes it tricky to eliminate the impact of the second factor.

At present, the impact of the duty ratio part on the accuracy of the traditional *dq* model has received little attention. It is well accepted that the frequency-coupling effect caused by the asymmetric *dq* control dynamics and the interaction with the time-periodic operation points is the crucial factor limiting the application of the traditional *dq* model [4], and it can be solved by the harmonic state space (HSS) modeling or the generalized *dq* modeling that are usually of high order [5].

Therefore, in this letter, the single-phase converter in railway vehicle-grid system using the SOGIs is taken for instance, and the accuracy of the traditional *dq* admittance modeling method is

Manuscript received 15 December 2023; revised 15 January 2024; accepted 30 January 2024. Date of publication 5 February 2024; date of current version 20 March 2024. This work was supported in part by the National Natural Science Foundation of China for the Research Project under Grant 52077188 and in part by the PolyU for the Intra-Faculty Interdisciplinary Project 1-WZ4L. *(Corresponding author: Siqi Bu.)*

Siqi Wu is with the Department of Electrical and Electronic Engineering, The Hong Kong Polytechnic University, Hong Kong (e-mail: wusiqi@my.swjtu.edu.cn).

Siqi Bu is with the Department of Electrical and Electronic Engineering, Shenzhen Research Institute, Research Centre for Grid Modernisation, The Hong Kong Polytechnic University, Hong Kong (e-mail: siqi.bu@polyu.edu.hk).

Zhigang Liu is with the School of Electrical Engineering, Southwest Jiaotong University, Chengdu 610032, China (e-mail: liuzg@swjtu.cn).

Color versions of one or more figures in this article are available at https://doi.org/10.1109/TPEL.2024.3362053.

Digital Object Identifier 10.1109/TPEL.2024.3362053

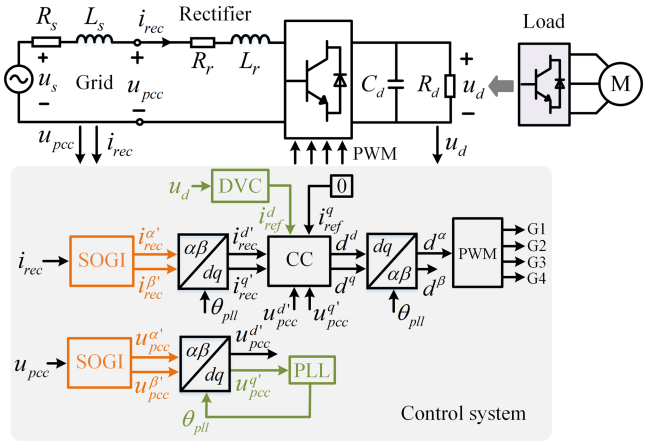

Fig. 1. Simplified single-phase vehicle-grid system.

further analyzed. It is revealed that the error from the duty ratio part originates from the asymmetric SOGIs, and is ultimately formed through the dimensionality reduction process from the actual control output to the power stage input (from 2-D to 1-D scalar, caused by the single-phase nature of the system), which usually is nonnegligible. To solve this issue, a novel idea to calibrate the traditional *dq* modeling method is proposed, which is easy to realize and also applicable to the converter with other types of QSG, thus, beneficial to the application of *dq* modeling in the single-phase ac systems.

II. Admittance of Single-Phase Converter

The railway vehicle-grid system simplified for the small-signal stability assessment in this letter is shown in Fig. 1 [1], [3]. The rectifier control system mainly includes the SOGIs, the dc voltage controller (DVC), the PLL, the current controller (CC) operating in the *dq* frame, and the equivalent auxiliary load R_d.

A. Traditional dq Admittance Model

According to the traditional *dq* modeling methodology and Fig. 1, the *dq* model of the closed-loop rectifier system including the power stage and all controllers is derived in Fig. 2 [3], which involves the ac operation trajectory at fundamental frequency ω_0 and the system small-signal dynamics at mirror frequencies ω_p and $2\omega_0-\omega_p$ (refers to $\alpha\beta$ frame) [6].

For clarification, the bold letters denote the space vectors, e.g., $\hat{\boldsymbol{d}} = [\hat{d}^d \quad \hat{d}^q]^{\mathrm{T}}$ and $\hat{\boldsymbol{i}}_{rec} = [\hat{i}^d_{rec} \quad \hat{i}^q_{rec}]^{\mathrm{T}}$, where the hat "^" denotes the small-signal variables. The transfer matrices in the purple and green areas represent the power stage and the controller models, respectively. Paths A and B in the colored lines represent the main impact paths of the $\alpha\beta$ components generated by the current and voltage SOGIs, respectively (elaborated later). Here, in the traditional *dq* model, the transfer functions $\boldsymbol{G}_i$ and $\boldsymbol{G}_u$ in these two paths are both identity matrices. $\boldsymbol{G}_{ce}$, $\boldsymbol{G}_{dei}$, and $\boldsymbol{G}_{ci}$ are provided in Appendix A for subsequent analysis. From Fig. 2, the rectifier admittance, i.e., the transfer function from the input voltage to the input current of the rectifier, can be derived.

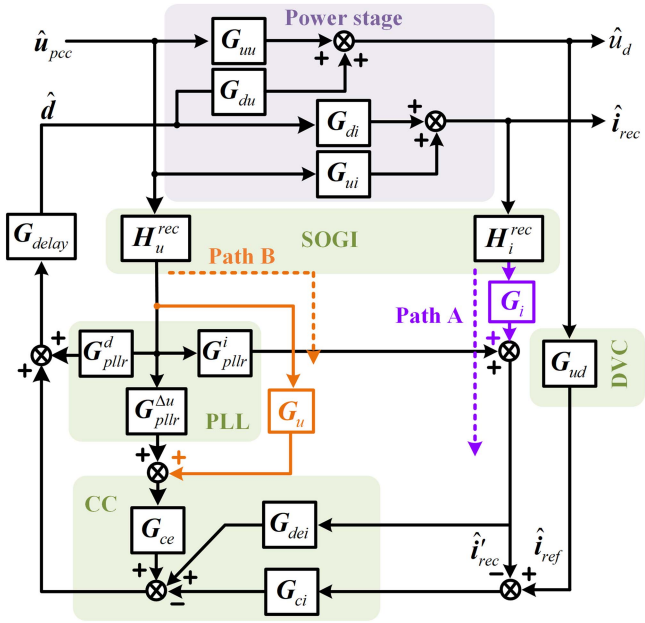

Fig. 2. Traditional *dq* model of the closed-loop rectifier system [3].

B. Benchmark for the Error Analysis and Accuracy Verification

The HSS model is a multi-input multi-output (MIMO) one built based on the harmonic balance principle [7], which describes the linear relationship between the Fourier coefficients of the input and the output signals of time-periodic systems in the phase domain ($\alpha\beta$ frame), through the harmonic transfer function matrices. The HSS admittance in the form of a large dimensional matrix can capture sufficient frequency coupling dynamics and be of high accuracy. Thus, in this letter, it is also derived based on Fig. 1 and taken as a benchmark. More importantly, the frequency coupling and control impact can be eliminated theoretically in the HSS and *dq* models, which, however, is unprocurable in the actual system. In this regard, it can provide a comprehensive comparison in a flexible way, facilitating the error analysis and accuracy validation of the *dq* admittance. To ensure adequate accuracy, the frequency coupling caused by the asymmetric *dq* control, the second harmonic of the dc voltage, and the third harmonic of ac variables are considered. The resulting HSS admittance is truncated to an $N = 3$ order matrix (involving the small-signal dynamics of input voltage and input current at ω_p and $\omega_p \pm 2\omega_0$).

C. SISO Equivalence

The *dq* and HSS models are both of MIMO characteristics. Hence, to facilitate the comparative analysis, they are equivalent to two single-input single-output (SISO) models in the phase domain based on the harmonic interactions of the grid and the rectifier in the closed-loop system [5], [6]. The equivalent SISO models of the rectifier *dq* and HSS admittances are denoted by Y^{dq}_{rec} and $\mathcal{Y}^{HSS}_{rec}$, respectively, which preserve all the coupling information involved in the original MIMO ones and will not sacrifice the accuracy of analytical results.

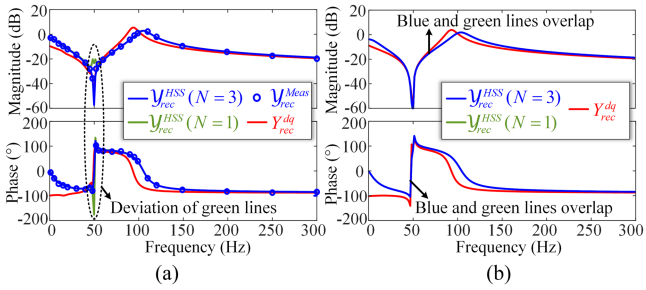

Fig. 3. Bode plots of *dq* and HSS admittance of rectifier. (a) Original rectifier system. (b) Rectifier system ignoring frequency couplings.

III. Deviation Introduced by Traditional *DQ* Modeling Method in Single-Phase AC Systems

In previous research, it is usually taken for granted that the system frequency-coupling effect should be the main culprit once the accuracy of the *dq* model is unsatisfactory. However, the asymmetric $\alpha\beta$ control, i.e., the asymmetric SOGIs, can also make a significant difference to the accuracy of the traditional *dq* model of single-phase ac systems, which will be clarified in this section. It is worth noting that the asymmetric $\alpha\beta$ control is not the root cause of frequency coupling in the phase domain, which differs from the impact of the asymmetric *dq* control. The parameters of the grid and the rectifier in Fig. 1 are listed in Table I in Appendix A.

A. Accuracy of Traditional dq Admittance

Fig. 3(a) compares the Bode plots of Y_{rec}^{dq}, $\mathcal{Y}_{rec}^{HSS}$, and the measured SISO admittance of the rectifier $\mathcal{Y}_{rec}^{meas}$ in MATLAB. The blue line represents the originally derived HSS model, and the green line represents the reduced-order HSS model ($N = 1$ order, only involves the small-signal dynamics at ω_p). Since the characteristics of Y_{rec}^{dq} and $\mathcal{Y}_{rec}^{HSS}$ above 300 Hz are close, they are not shown here for discussion. As can be seen, the admittance $\mathcal{Y}_{rec}^{HSS}$ in the blue line matches well with the measured one $\mathcal{Y}_{rec}^{meas}$in blue circles. Thus, the accuracy of the derived 3-order HSS model is validated. However, the *dq* model Y_{rec}^{dq} presents obvious deviation around 100 Hz, which will inevitably lead to inaccurate stability analytical results. For the reduced-order HSS model $\mathcal{Y}_{rec}^{HSS}$ in the green line, its deviation is mainly around 50 Hz, implying the frequency coupling here is most significant.

B. Factors Affecting the Traditional dq Admittance Accuracy

1) Impact of Frequency-Coupling Effect: If the dc voltage of the rectifier is assumed to be constant (equal to the reference value 3600 V) and the dynamics from PLL and DVC are ignored, the power stage and the control system both become linear systems without frequency couplings. In this scenario, the corresponding *dq* model Y_{rec}^{dq} and HSS model $\mathcal{Y}_{rec}^{HSS}$ are drawn in Fig. 3(b). The reduced-order HSS model $\mathcal{Y}_{rec}^{HSS}(N = 1)$ in green overlaps with the original 3-order model $\mathcal{Y}_{rec}^{HSS}(N = 3)$, as expected. However, the deviation of the *dq* model still exists, which prompts us to further explore the key culprit causing this error.

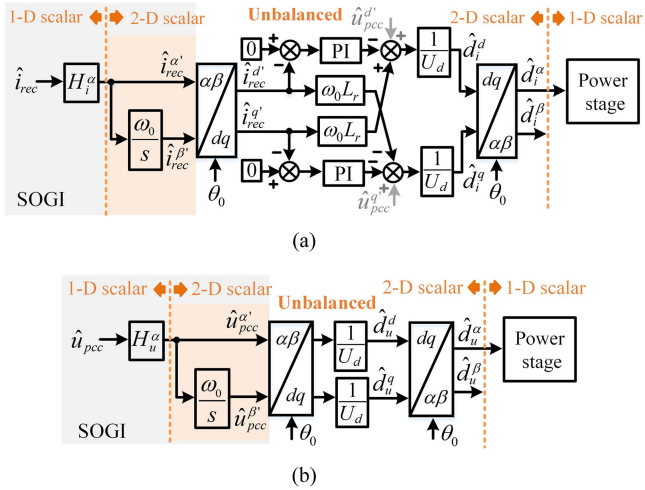

Fig. 4. Main impact paths of the unbalanced components generated by the SOGIs in the rectifier control system. (a) Path A depicting the impact of current SOGI. (b) Path B depicting the impact of voltage SOGI.

2) Impact of Asymmetric SOGIs: There is only one phase in the single-phase system. Thus, to realize *dq*-frame immittance modeling or *dq*-frame control, the quadrature components in β frame should be constructed for Park transformation. However, the β components constructed by the SOGIs inevitably own nonideal amplitudes, which means that the $\alpha\beta$ components generated by SOGI are unbalanced. As shown in Fig. 1, there are two SOGIs used in the rectifier control system. Since the small-signal model is built on the linearized system, the impact of the voltage SOGI and the current SOGI on the final duty ratio signals is superposable and can be analyzed separately.

As shown in Fig. 3(b), the deviation of the *dq* model still exists when the PLL dynamics are ignored. In this regard, the impact of PLL is not dominant. The main impact paths of the unbalanced components generated by the voltage and current SOGIs in the concerned frequency range (around 100 Hz) are Path A and Path B, respectively, as shown in Fig. 4, where the input phase for Park and inverse Park transform is set to the steady-state value θ_0. H_i^α and H_u^α are two bandpass filters brought by SOGIs. Obviously, the nonideal β components are initially introduced by the delay block ω_0/s of SOGI. The contributed $\alpha\beta$ duty ratio signals of Path A and Path B are respectively defined as $\hat{d}_i^\alpha$ and $\hat{d}_i^\beta$ as well as $\hat{d}_u^\alpha$ and $\hat{d}_u^\beta$. According to Fig. 4, the output duty ratio signals in both subfigures will also be unbalanced. To facilitate understanding, the concept of "positive" sequence (β component lags α component by 90°) and "negative" sequence (β component leads α component by 90°) is adopted below to explain how the unbalanced duty ratio signals affect the accuracy of the traditional *dq* model.

Fig. 4(a) is taken for instance. According to the principle of *dq* modeling [1], [2], [3], only the "positive" sequence components at mirror frequencies can be involved in the *dq* model. Assuming the small signal $\hat{\imath}_{rec}^{\alpha'}$ is at frequency ω_p, the unbalanced duty ratios $\hat{d}_i^\alpha$ and $\hat{d}_i^\beta$ at ω_p will be generated, which consist of both "positive" and "negative" sequence components (see Fig. 5). In the *dq* model of the control system, the "positive" sequence components in $\hat{d}_i^\alpha$ and $\hat{d}_i^\beta$ are captured. However, as shown in

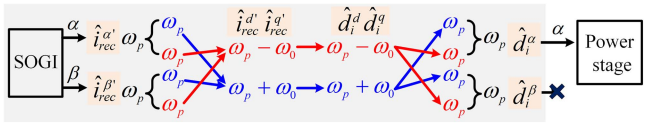

Fig. 5. "Positive" (in red) and "negative" sequence (in blue) flows in Path A.

Fig. 4(a), the actual single-phase power stage only adopts the α duty ratio $\hat{d}_i^{\alpha}$ as its input. Thus, when we build the dq model of the power stage, the β duty ratio is artificially defined as the one lagging $\hat{d}_i^{\alpha}$ by 90°. In this regard, $\hat{d}_i^{\alpha}$ is directly regarded as the α-axis "positive" sequence component. As a result, the "positive" sequence duty ratio components considered in the dq models of the control system and the power stage are different, and a transfer function depicting the transitive relation between these two "positive" sequence components (depicting the dimensionality reduction process) is necessary for connecting the control system and the power stage. However, it is missed in the traditional dq model, which leads to the deviation in Fig. 3.

IV. Optimized *DQ* Modeling Method

In this section, the transfer function matrices $\boldsymbol{G}_{ip}$ and $\boldsymbol{G}_{up}$, respectively, for capturing the dimensionality reduction process of the duty ratio signals in Paths A and B, are derived to bridge the dq models of the control system and power stage, for calibration.

A. Unbalanced Duty Ratio Signals in Path A and Path B

First, Path A in Fig. 4(a) is analyzed. Suppose the frequency-domain expression of the small signal $\hat{i}_{rec}^{\alpha'}$ at frequency ω_p is

$$\hat{i}_{rec}^{\alpha'}(\omega) = I_p\pi\delta(\omega+\omega_p) + I_p\pi\delta(\omega-\omega_p) \triangleq \delta^+(\omega)+\delta^-(\omega) \tag{1}$$

where I_p is the signal magnitude. δ is the unit impulse function.

Then, the unbalanced $\alpha\beta$ currents generated by the SOGI are

$$\hat{\boldsymbol{i}}_{rec}^{\alpha\beta'} = \begin{bmatrix} \hat{i}_{rec}^{\alpha'}(\omega) \\ \hat{i}_{rec}^{\beta'}(\omega) \end{bmatrix} = \begin{bmatrix} 1 \\ k_{lag}(\mathrm{j}\omega) \end{bmatrix} \left(\delta^+(\omega)+\delta^-(\omega)\right) \tag{2}$$

where $k_{lag}(\mathrm{j}\omega) = \omega_0/(\mathrm{j}\omega)$.

Based on the Park transform and frequency shifting property of the Fourier transform, the $\alpha\beta$ currents in (2) are converted to the dq frame, and we can get the current $\hat{\boldsymbol{i}}_{rec}^{dq'} = [\hat{i}_{rec}^{d'} \quad \hat{i}_{rec}^{q'}]^{\mathrm{T}}$ as

$$\hat{\boldsymbol{i}}_{rec}^{dq'} = \underbrace{\frac{1}{2}\begin{bmatrix} A(\mathrm{j}\omega) & B(\mathrm{j}\omega) \\ -\mathrm{j}A(\mathrm{j}\omega) & \mathrm{j}B(\mathrm{j}\omega) \end{bmatrix}}_{\boldsymbol{G}_{lag}(\mathrm{j}\omega)=\boldsymbol{G}_{sogi}(\mathrm{j}\omega).\boldsymbol{K}} \left(\begin{bmatrix} \delta^-(\omega+\omega_0) \\ \delta^+(\omega-\omega_0) \end{bmatrix} + \begin{bmatrix} \delta^+(\omega+\omega_0) \\ \delta^-(\omega-\omega_0) \end{bmatrix} \right) \tag{3}$$

where $A(\mathrm{j}\omega) = \mathrm{j}-k_{lag}(\mathrm{j}(\omega+\omega_0))$ and $B(\mathrm{j}\omega) = -\mathrm{j}-k_{lag}(\mathrm{j}(\omega-\omega_0))$. $\boldsymbol{G}_{sogi}(\mathrm{j}\omega)$ is the dq model for the SOGI controller in the orange area in Fig. 4. $\boldsymbol{K}$ is a constant coefficient matrix, as in Appendix A. The current in blue is transformed from the "negative" sequence component in (2), whose flow path is shown in Fig. 5 (in blue).

Then, according to the CC control in Fig. 4(a) and (3), we get

$$\begin{aligned} \hat{\boldsymbol{d}}_i^{dq} &= \frac{1}{U_d}\begin{bmatrix} G_{\mathrm{PI}}(\mathrm{j}\omega) & \omega_0 L_r \\ -\omega_0 L_r & G_{\mathrm{PI}}(\mathrm{j}\omega) \end{bmatrix} \hat{\boldsymbol{i}}_{rec}^{dq'} \\ &= \left(\boldsymbol{G}_{dei}(\mathrm{j}\omega)+\boldsymbol{G}_{ci}(\mathrm{j}\omega)\right)\hat{\boldsymbol{i}}_{rec}^{dq'} \\ &\triangleq \begin{bmatrix} C_i(\mathrm{j}\omega) & D_i(\mathrm{j}\omega) \\ -\mathrm{j}C_i(\mathrm{j}\omega) & \mathrm{j}D_i(\mathrm{j}\omega) \end{bmatrix} \left(\begin{bmatrix} \delta^-(\omega+\omega_0) \\ \delta^+(\omega-\omega_0) \end{bmatrix} + \begin{bmatrix} \delta^+(\omega+\omega_0) \\ \delta^-(\omega-\omega_0) \end{bmatrix} \right) \end{aligned} \tag{4}$$

where $\boldsymbol{G}_{dei}(\mathrm{j}\omega)$ and $\boldsymbol{G}_{ci}(\mathrm{j}\omega)$ are the frequency-domain forms of the defined matrices in Fig. 2. $G_{\mathrm{PI}}(\mathrm{j}\omega)$ denotes the PI control in CC.

Finally, performing inverse Park transform on (4), the $\alpha\beta$-frame unbalanced duty ratio $\hat{\boldsymbol{d}}_i^{\alpha\beta} = [\hat{d}_i^{\alpha} \quad \hat{d}_i^{\beta}]^{\mathrm{T}}$ is derived as

$$\hat{\boldsymbol{d}}_i^{\alpha\beta} = \begin{bmatrix} \underbrace{\mathrm{j}D_i(\mathrm{j}(\omega+\omega_0)) - \mathrm{j}C_i(\mathrm{j}(\omega-\omega_0))}_{M_i^{\alpha}(\mathrm{j}\omega)} \\ \underbrace{-D_i(\mathrm{j}(\omega+\omega_0)) - C_i(\mathrm{j}(\omega-\omega_0))}_{M_i^{\beta}(\mathrm{j}\omega)} \end{bmatrix} \cdot \left(\delta^+(\omega)+\delta^-(\omega)\right). \tag{5}$$

According to (5), the output unbalanced duty ratio is at the same frequency ω_p with the original input current perturbation. Hence, no frequency coupling is introduced. Note that the time delay is on both α and β channels, thus not affecting the imbalance. In addition, from (3)–(5), it is found that the key elements C_i and D_i in (5) can be directly obtained according to the product of ($\boldsymbol{G}_{dei}$+$\boldsymbol{G}_{ci}$) (see Fig. 2, the transfer matrices of CC in Path A in the traditional dq model) and $\boldsymbol{G}_{lag}$ (see (3), related to the delay block of SOGI), thus, no need to derive from Fig. 4(a) if the traditional dq model is available. In this regard, the contributed unbalanced duty ratio signals of Path B shown in Fig. 4(b) can be formulated similarly according to the product of $\boldsymbol{G}_{ce}$ (see Fig. 2, CC model in Path B) and $\boldsymbol{G}_{lag}$, and the inverse Park transformation [refer to the transform from (4) to (5)].

For clarification, the "positive" sequence duty ratio involved in the dq models of the control system and the power stage in Path A are respectively defined as $\hat{\boldsymbol{d}}_{i\_con}^{dq}$ and $\hat{\boldsymbol{d}}_{i\_pow}^{dq}$, while those in Path B are, respectively, defined as $\hat{\boldsymbol{d}}_{u\_con}^{dq}$ and $\hat{\boldsymbol{d}}_{u\_pow}^{dq}$.

B. Basic Idea to Derive the Expressions of $\boldsymbol{G}_{ip}$ and $\boldsymbol{G}_{up}$

In general, $\boldsymbol{G}_{ip}$ and $\boldsymbol{G}_{up}$ can be obtained in two different ways based on the derived expressions of the unbalanced duty ratio signals. Take $\boldsymbol{G}_{ip}$ in Path A for instance. The "positive" sequence component marked in black in (4) is $\hat{\boldsymbol{d}}_{i\_con}^{dq}$, and the α-axis "positive" sequence component in $\hat{\boldsymbol{d}}_{i\_pow}^{dq}$ is equal to $\hat{d}_i^{\alpha}$ in (5). Therefore, the first approach that naturally comes to mind is to extract $\hat{\boldsymbol{d}}_{i\_con}^{dq}$ and $\hat{\boldsymbol{d}}_{i\_pow}^{dq}$ based on (4) and (5), and the ratio of them in s-domain is $\boldsymbol{G}_{ip}$, as shown in Appendix B.

This is similar to the derivation of the dq model $\boldsymbol{G}_{sogi}$ for the SOGI controller in the orange area of Fig. 4 since the "positive"

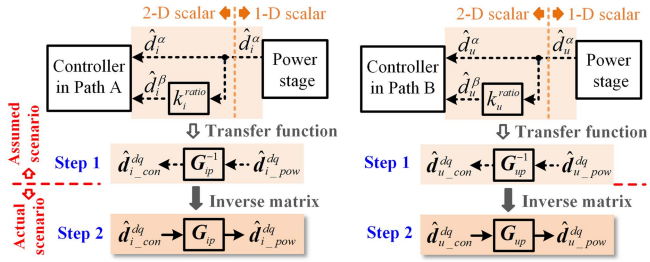

Fig. 6. Basic idea for derivation of $\boldsymbol{G}_{ip}$ and $\boldsymbol{G}_{up}$, where a hypothetical bridge for connecting the power stage and control system is built for better understanding.

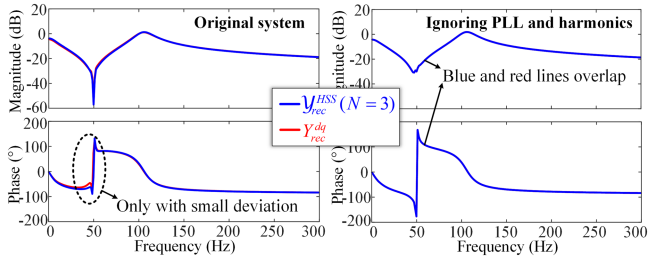

Fig. 7. Bode plots of optimized dq model Y_{rec}^{dq} and HSS model $\mathcal{Y}_{rec}^{HSS}$.

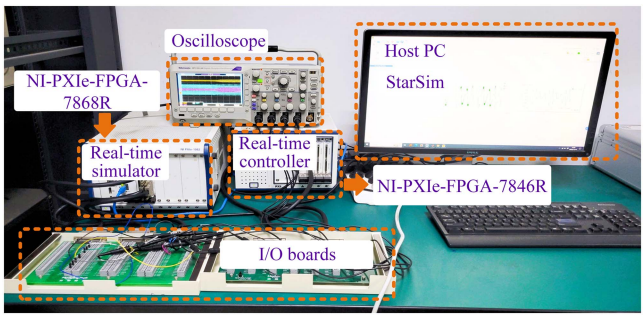

Fig. 8. Controller HIL simulation platform.

sequence components in its input (1-D) and output (2-D, unbalanced) signals also need to be extracted for calculation. In this regard, recalling Fig. 4, a very interesting phenomenon can be noticed. The signal dimensionality is first raised by SOGI and then reduced at the duty ratio part. If we look from the power stage to the control system, it is a dimensionality ascending process, similar to that in SOGI. As indicated in Fig. 4 [or (3)], $\boldsymbol{G}_{sogi}$ is determined by the delay block ω_0/s [see (2), k_{lag}] of SOGI, which is the ratio of its β and α output signals. Thus, inspired by this, we can consider the derivation of $\boldsymbol{G}_{ip}$ and $\boldsymbol{G}_{up}$ from another novel perspective, as shown in Fig. 6 , where a hypothetical bridge between the power stage and the control system is built. k_i^{ratio} and k_u^{ratio} denote the ratio of the β and α signals output by the control system in Path A and Path B, respectively. In this way, $\boldsymbol{G}_{ip}$ and $\boldsymbol{G}_{up}$ can be formulated directly, which are of the same form as the inverse of $\boldsymbol{G}_{sogi}$ [see (3)], and are respectively determined by k_i^{ratio} and k_u^{ratio}. The hypothesis in Fig. 6 is reasonable, as it does not change the original relation between the 2-D control output and the 1-D power stage input, which facilitates a better understanding of $\boldsymbol{G}_{ip}$ and $\boldsymbol{G}_{up}$.

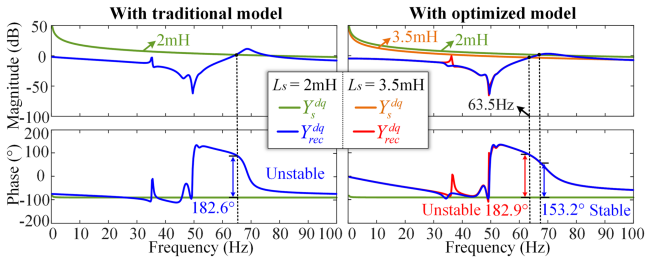

Fig. 9. Bode plots for stability analysis when $k_{Pi} = 1.9$.

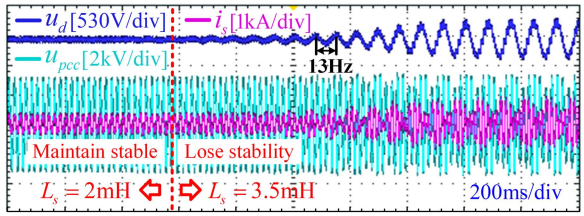

Fig. 10. Waveforms when $k_{Pi} = 1.9$ and L_s is increased from 2 to 3.5 mH.

According to (5), the ratio k_i^{ratio} in s domain is calculated as the first equation in (6), where $s = \mathrm{j}\omega$. Similarly, k_u^{ratio} can be obtained. Nevertheless, we can also directly observe from Fig. 4(b) that k_u^{ratio} is equal to the ratio of $\hat{u}_{pcc}^{\beta'}$ and $\hat{u}_{pcc}^{\alpha'}$, shown as

$$k_i^{ratio}(s) = \frac{M_i^{\beta}(s)}{M_i^{\alpha}(s)} \text{ and } k_u^{ratio}(s) = \frac{\hat{d}_u^{\beta}(s)}{\hat{d}_u^{\alpha}(s)} = \frac{\hat{u}_{pcc}^{\beta'}(s)}{\hat{u}_{pcc}^{\alpha'}(s)} = \frac{\omega_0}{s}. \tag{6}$$

The expression of $\boldsymbol{G}_{sogi}$ is known [see (3)], and its inverse is in (7). If the ratio k_{lag} in (7) is respectively replaced with $k_i^{ratio}$and k_u^{ratio}in (6), the right side of (7) will be, respectively, equal to $\boldsymbol{G}_{ip}$ and $\boldsymbol{G}_{up}$.

$$\boldsymbol{G}_{sogi}^{-1} = \boldsymbol{K}\boldsymbol{G}_{lag}^{-1} = \begin{bmatrix} G_a(s) & G_b(s) \\ -G_b(s) & G_a(s) \end{bmatrix}^{-1} \tag{7}$$

wherein $\begin{cases} G_a(s) = (2 + \mathrm{j}k_{lag}(s + \mathrm{j}\omega_0) - \mathrm{j}k_{lag}(s - \mathrm{j}\omega_0))/4 \\ G_b(s) = (-k_{lag}(s + \mathrm{j}\omega_0) - k_{lag}(s - \mathrm{j}\omega_0))/4 \end{cases}$.

The coefficient $1/U_d$ on d and q channels in Path B [see Fig. 4(b)] has no impact on k_u^{ratio}, thus no impact on $\boldsymbol{G}_{up}$. Besides, since the ratio k_u^{ratio} is equal to k_{lag}, $\boldsymbol{G}_{up}$ is the inverse matrix of $\boldsymbol{G}_{sogi}$. When $\boldsymbol{G}_{up}$ is added to Path B for calibration, the impact of these two matrices will be canceled, indicating $\boldsymbol{G}_{sogi}$ essentially has no effect on the dynamics of Path B. Thus, the entire model on Path B is simplified instead. If needed, the analytic expression of $\boldsymbol{G}_{ip}$ can be easily solved by virtue of a similar product form as $\boldsymbol{K}\boldsymbol{G}_{lag}^{-1}$ in (7).

C. Accuracy of the Optimized dq Admittance With $\boldsymbol{G}_{ip}$ and $\boldsymbol{G}_{up}$

In consequence, the dq model of the rectifier in Fig. 2 can be optimized by replacing the original identity matrices $\boldsymbol{G}_i$ and $\boldsymbol{G}_u$ with the derived $\boldsymbol{G}_{ip}$ and $\boldsymbol{G}_{up}$, respectively. This is a concise representation since the matrices $\boldsymbol{G}_{up}$ and $\boldsymbol{G}_{ce}$ (see Fig. 2), as well as $\boldsymbol{G}_{ip}$ and ($\boldsymbol{G}_{dei}$+$\boldsymbol{G}_{ci}$) [see Fig. 2 or (4)] both satisfy the multiplication commutative law. Note that the DVC (see Fig. 1)

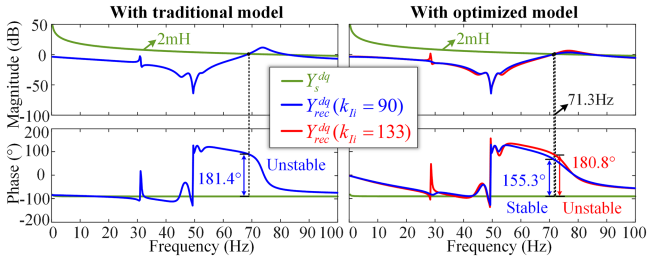

Fig. 11. Bode plots for stability analysis when $k_{Pi} = 2.6$, and k_{Ii} is increased to 90 or 133.

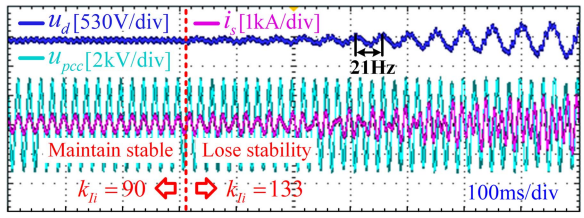

Fig. 12. Waveforms when $k_{Pi} = 2.6$, and k_{Ii} is increased from 90 to 133.

is an asymmetric controller in the *dq* frame, and the mirror-frequency duty ratios generated by it are always balanced.

For verification, the optimized *dq* model is compared with the accurate HSS model (benchmark) in Fig. 7. The optimized *dq* model is very close to the HSS model. When the PLL impact and the steady-state harmonics are ignored, the two models almost coincide (the blue and red lines overlap), as expected. Therefore, the nonnegligible error of the *dq* model in Fig. 3(a) stems from the asymmetric SOGIs and is ultimately formed by the duty ratio dimensionality reduction. The proposed optimization approach can eliminate this error effectively. If another type of QSG, e.g., the transfer delay, is used, we only need to replace the delay model ω_0/s in (6) with the new delay $e^{-s/(4f_0)}$.

V. Stability Analysis and Hardware-in-the-Loop (HIL) Verification

To further verify the accuracy of the optimized *dq* modeling method, the system stability is evaluated based on the Bode plots of the grid SISO admittance $Y_s^{dq} = 1/(R_s + sL_s)$ and the rectifier admittance Y_{rec}^{dq}, and then validated via the controller HIL simulations on the platform shown in Fig. 8. The parameter set of the grid and the rectifier listed in Table I is taken as the base case, which represents a small signal stable condition. The control parameters can be varied via the control algorithm in the industrial digital controller in run mode, whereas the grid variation can be achieved through the physical switching function of the breakers in the real-time simulator.

As shown in Fig. 9, with the traditional *dq* model, the system is predicted to be unstable when the rectifier CC parameter k_{Pi} is decreased to 1.9. However, the optimized *dq* model in the right figure (see the blue line) predicts a stable system under the same parameters. As shown by the red and orange lines, when k_{Pi} is kept at 1.9, and the grid inductance L_s is switched from 2 to 3.5 mH, the system will lose stability. The frequency at the amplitude intersection is 63.5 Hz, indicating the oscillation frequency of dc voltage u_d will be 13.5 Hz. The analytical results based on the optimized *dq* model match well with the HIL results in Fig. 10. For sufficient validation, the stability analysis is conducted under another set of CC parameters. As shown in Figs. 11 and 12, the system stability and oscillation frequency can be accurately evaluated by the optimized *dq* model, whereas the traditional one brings obvious deviation. Note that the SISO equivalence is realized in the closed-loop scenario. Thus, the grid admittance is involved in the expression of Y_{rec}^{dq} [see (A8) in Appendix C] and its variation can affect Y_{rec}^{dq}, as indicated in the right subfigure of Fig. 9.

VI. Conclusion

In this letter, the impact of asymmetric SOGIs on the traditional *dq* admittance accuracy of the single-phase converter in railway vehicle-grid system is revealed. It is clarified that the asymmetric SOGIs can introduce unbalanced duty ratio signals in the control system, which eventually causes the deviation of the traditional *dq* model under the signal dimensionality reduction operation from the control system to the power stage. To solve this issue, an optimization method for the traditional *dq* admittance is proposed, wherein the transfer function matrices for describing the dimensionality reduction operation are introduced to bridge the *dq* models of the control system and the power stage accurately. This optimization can be easily achieved based on the existing *dq* models, and the idea to alleviate the impact of SOGIs is also applicable to other asymmetric $\alpha\beta$ controllers, especially the commonly used QSGs, such as the transfer delay. Therefore, this research provides a better understanding of *dq* modeling method and facilitates its application in single-phase ac systems.

Appendix

A. Matrix Expressions and Parameters of the Rectifier and Grid

TABLE I
Parameters of the Grid and Rectifier

Model	Parameters	Values	Parameters	Values
Grid	U_{srms}	1947 V	R_s	0.001 Ω
	f_0	50 Hz	L_s	2 mH
Rectifier	f_s	2500 Hz	U_d	3600 V
	C_d	9 mF	R_d	50 Ω
	R_r	0.15 Ω	L_r	5.4 mH
	T_{delay}	3e-4 s	k_{Pu}, k_{Iu}	0.2, 5
	k_{Pi}, k_{Ii}	6, 50	k_{Ppll}, k_{Ipll}	0.7, 25

The expressions of $\boldsymbol{G}_{ce}$, $\boldsymbol{G}_{dei}$, and $\boldsymbol{G}_{ci}$ in Fig. 2 and $\boldsymbol{K}$ in (3) are

$$\boldsymbol{G}_{ce} = \frac{1}{U_d}\begin{bmatrix}1 & 0\\ 0 & 1\end{bmatrix},\ \boldsymbol{G}_{dei} = \frac{1}{U_d}\begin{bmatrix}0 & \omega_0 L_r\\ -\omega_0 L_r & 0\end{bmatrix},$$
$$\boldsymbol{K} = \begin{bmatrix}\mathrm{j} & -\mathrm{j}\\ 1 & 1\end{bmatrix} \tag{A1}$$

$$\boldsymbol{G}_{ci} = \frac{1}{U_d}\begin{bmatrix} k_{Pi}+k_{Ii}/s & 0 \\ 0 & k_{Pi}+k_{Ii}/s \end{bmatrix} \triangleq \frac{1}{U_d}\begin{bmatrix} G_{\mathrm{PI}}(s) & 0 \\ 0 & G_{\mathrm{PI}}(s) \end{bmatrix}. \tag{A2}$$

B. Derivation of $\boldsymbol{G}_{ip}$ Based on Expressions of $\hat{\boldsymbol{d}}^{dq}_{i\_con}$ and $\hat{\boldsymbol{d}}^{dq}_{i\_pow}$

The "positive" sequence duty ratio $\hat{\boldsymbol{d}}^{dq}_{i\_con}$ extracted directly from (4) is

$$\hat{\boldsymbol{d}}^{dq}_{i\_con} = \begin{bmatrix} C_i(\mathrm{j}\omega) & D_i(\mathrm{j}\omega) \\ -\mathrm{j}C_i(\mathrm{j}\omega) & \mathrm{j}D_i(\mathrm{j}\omega) \end{bmatrix}\begin{bmatrix} \delta^-(\omega+\omega_0) \\ \delta^+(\omega-\omega_0) \end{bmatrix}. \tag{A3}$$

According to (5), the $\alpha\beta$-frame "positive" sequence component considered in the *dq* model of the power stage is formulated as follows:

$$\hat{\boldsymbol{d}}^{\alpha\beta}_{i\_pow} = M_i^{\alpha}(\mathrm{j}\omega)\begin{bmatrix} \delta^+(\omega)+\delta^-(\omega) \\ \mathrm{j}\delta^+(\omega)-\mathrm{j}\delta^-(\omega) \end{bmatrix} \tag{A4}$$

where the α component is equal to that in (5), and the β component is an ideal 90° lagging term.

Converting (A4) from the $\alpha\beta$ frame to the *dq* frame yields

$$\hat{\boldsymbol{d}}^{dq}_{i\_pow} = \boldsymbol{K}\begin{bmatrix} M_i^{\alpha}(\mathrm{j}(\omega+\omega_0)) & 0 \\ 0 & M_i^{\alpha}(\mathrm{j}(\omega-\omega_0)) \end{bmatrix} \cdot \begin{bmatrix} \delta^-(\omega+\omega_0) \\ \delta^+(\omega-\omega_0) \end{bmatrix}. \tag{A5}$$

Finally, the transfer function $\boldsymbol{G}_{ip}$ from $\hat{\boldsymbol{d}}^{dq}_{i\_con}$ to $\hat{\boldsymbol{d}}^{dq}_{i_pow}$in s-domain can be calculated, as in the following equation, where $s = \mathrm{j}\omega$. It is equal to the result derived based on the second approach (see the idea in Fig. 6)

$$\boldsymbol{G}_{ip} = \boldsymbol{K}\begin{bmatrix} M_i^{\alpha}(s+\mathrm{j}\omega_0) & 0 \\ 0 & M_i^{\alpha}(s-\mathrm{j}\omega_0) \end{bmatrix} \cdot \begin{bmatrix} C_i(s) & D_i(s) \\ -\mathrm{j}C_i(s) & \mathrm{j}D_i(s) \end{bmatrix}^{-1}. \tag{A6}$$

C. SISO Equivalence of dq Admittance

To realize the SISO equivalence, the *dq* model of the rectifier is transformed to the $\alpha\beta$ frame first, yielding (A7). Then, based on the SISO equivalence principle and (A7), Y^{dq}_{rec} is derived as (A8) [5].

$$\begin{bmatrix} \hat{i}_{rec(\omega_p)} \\ \hat{i}_{rec(\omega_p-2\omega_0)} \end{bmatrix} = \begin{bmatrix} Y^{dq}_{11}(s) & Y^{dq}_{12}(s) \\ Y^{dq}_{21}(s) & Y^{dq}_{22}(s) \end{bmatrix}\begin{bmatrix} \hat{u}_{pcc(\omega_p)} \\ \hat{u}_{pcc(\omega_p-2\omega_0)} \end{bmatrix} \tag{A7}$$

wherein Y^{dq}_{11} and Y^{dq}_{22} describe the relation of the input voltage u_{pcc} and input current i_{rec} at the same frequency, while the nondiagonal elements Y^{dq}_{12} and Y^{dq}_{21} are the frequency-coupling terms.

$$Y^{dq}_{rec}(s) = Y^{dq}_{11}(s) - Y^{dq}_{12}(s)\,Y^{dq}_{21}(s)\Big/\left(Y^{dq}_{s}(s-\mathrm{j}2\omega_0)+Y^{dq}_{22}(s)\right) \tag{A8}$$

where $Y^{dq}_{s}(s-\mathrm{j}2\omega_0)$ is the frequency shift version of the grid SISO admittance $Y^{dq}_{s}(s)$.

REFERENCES

[1] Y. Liao, Z. Liu, H. Zhang, and B. Wen, "Low-frequency stability analysis of single-phase system with *dq*-frame impedance approach—Part II: Stability and frequency analysis," *IEEE Trans. Ind. Appl.*, vol. 54, no. 5, pp. 4999–5011, Sep./Oct. 2018.

[2] Y. Zhou, H. Hu, X. Yang, Z. Meng, and Z. He, "Impacts of quadrature signal generation-based PLLs on low-frequency oscillation in an electric railway system," *IEEE Trans. Transp. Electrific.*, vol. 7, no. 4, pp. 3124–3136, Dec. 2021.

[3] S. Wu and Z. Liu, "Low-frequency stability analysis of vehicle-grid system with active power filter based on *dq*-frame impedance," *IEEE Trans. Power Electron.*, vol. 36, no. 8, pp. 9027–9040, Aug. 2021.

[4] X. Meng et al., "Conversion and SISO equivalence of impedance model of single-phase converter in electric multiple units," *IEEE Trans. Transp. Electrific.*, vol. 9, no. 1, pp. 1363–1378, Mar. 2023.

[5] C. Zhang, M. Molinas, S. Føyen, J. A. Suul, and T. Isobe, "Harmonic domain SISO equivalent impedance modeling and stability analysis of a single-phase grid connected VSC," *IEEE Trans. Power Electron.*, vol. 35, no. 9, pp. 9770–9783, Sep. 2020.

[6] X. Wang, L. Harnefors, and F. Blaabjerg, "Unified impedance model of grid-connected voltage-source converters," *IEEE Trans. Power Electron.*, vol. 33, no. 2, pp. 1775–1787, Feb. 2018.

[7] N. M. Wereley, "Analysis and control of linear periodically time varying systems," Ph.D. dissertation, Dept. Aeronaut. Astronaut., MIT, Cambridge, MA, USA, 1991.